Journal of Achievements in Materials and Manufacturing Engineering
VOLUME 54
ISSUE 2
October
2012

Fracture toughness of advanced alumina ceramics and alumina matrix composites used for cutting tool edges

M. Szutkowska*
Centre of Materials Engineering and Sintering Techniques,
Institute of Advanced Manufacturing Technology,
ul. Wrocławska 37a, 30-011 Kraków, Poland
* Corresponding e-mail address: magdalena.szutkowska@ios.krakow.pl

Received 19.08.2012; published in revised form 01.10.2012

Materials

ABSTRACT

Purpose: Specific characteristics in fracture toughness measurements of advanced alumina ceramics and alumina matrix composites with particular reference to α-Al_2O_3, Al_2O_3-ZrO_2, Al_2O_3-ZrO_2-TiC and Al_2O_3-Ti(C,N) has been presented.
Design/methodology/approach: The present study reports fracture toughness obtained by means of the conventional method and direct measurements of the Vickers crack length (DCM method) of selected tool ceramics based on alumina: pure alumina, alumina-zirconia composite with unstabilized and stabilized zirconia, alumina–zirconia composite with addition of TiC and alumina–nitride-carbide titanium composite with 2wt% of zirconia. Specimens were prepared from submicro-scale trade powders. Vicker's hardness (HV1), fracture toughness (K_{IC}) at room temperature, the indentation fracture toughness, Young's modulus and apparent density were also evaluated. The microstructure was observed by means of scanning electron microscopy (SEM).
Findings: The lowest value of K_{IC} is revealed by pure alumina ceramics. The addition of (10 wt%) unstabilized zirconia to alumina or a small amount (5 wt%) of TiC to alumina–zirconia composite improve fracture toughness of these ceramics in comparison to alumina ceramics. Alumina ceramics and alumina-zirconia ceramics reveal the pronounced character of R-curve because of an increasing dependence on crack growth resistance with crack extension as opposed to the titanium carbide-nitride reinforced composite based on alumina. R-curve has not been observed for this composite.
Practical implications: The results show the method of fracture toughness improvement of alumina tool ceramics.
Originality/value: Taking into account the values of fracture toughness a rational use of existing ceramic tools should be expected.
Keywords: Alumina ceramics; Alumina matrix composites; Fracture toughness; Indentation fracture toughness; Vickers hardness

Reference to this paper should be given in the following way:
M. Szutkowska, Fracture toughness of advanced alumina ceramics and alumina matrix composites used for cutting tool edges, Journal of Achievements in Materials and Manufacturing Engineering 54/2 (2012) 202-210.

1. Introduction

The major goal of current ceramic research and development is to produce tough, strong ceramics that perform reliably. Recently the increasing interest in alumina ceramics has been observed because of their excellent resistance to wear, high hardness, resistance to corrosion, chemical stability behavior, good mechanical properties at high temperatures and relatively cheap technology of production [1,2,3]. The primary disadvantage of ceramic materials is their brittle nature characterized by low fracture toughness (Fig. 1) [4].

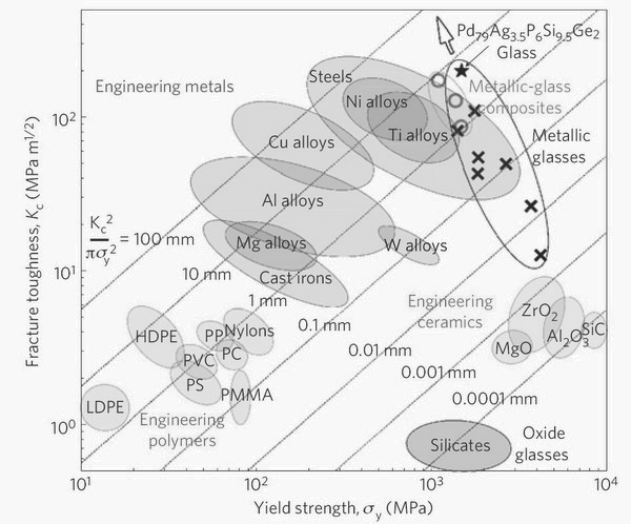

Fig. 1. Fracture toughness (K_C) against yield strength (σ_y) for engineering materials [4]

Fracture toughness, often perceived as the limiting factor for ceramics applications, is being improved to make ceramics competitive as engineering materials. Using fracture mechanics techniques, the critical stress-intensity factor K_{IC} (fracture toughness) of the material, is determined regardless of the nature of the material [5]. Fracture toughness is a measure of a material's ability to resist fracture in the presence of a crack. Precise design methodologies and modeling are therefore necessary to help predict the performance of ceramics. Such a modeling requires statistically valid data about fracture toughness, wear, strength and hardness. [6]. Overall magnitude of the stress field around the crack is controlled by parameter K, called *stress intensity,* which is proportional to the uniform tension applied to the material. Three linearly independent cracking modes are used in fracture mechanics. These load types are categorized as mode I, II, or III as shown in the graph (Fig. 2). Mode I, shown to the left, is an opening (tensile) mode where the crack surfaces move directly apart. The fracture of brittle ceramics is usually controlled by mode I (opening).

This critical value determined for mode I loading in plane strain is referred to as critical fracture toughness (K_{IC}) of the material. A simple dimensional analysis of a body containing a crack of length 2a and subject to the applied stresses shows that the critical stress intensification at the crack tip K_{IC} is:

$$K_{IC} = Y\sigma_c\sqrt{\pi a}_c \text{ s} \quad (1)$$

where: K_{IC} is the plane-strain fracture toughness, σ_c is the critical applied stress that will cause failure, $Y=f(a/W)$ is a constant related to the sample's geometry, a_c is the critical crack length for edge cracks or one half of the critical crack length for an internal crack.

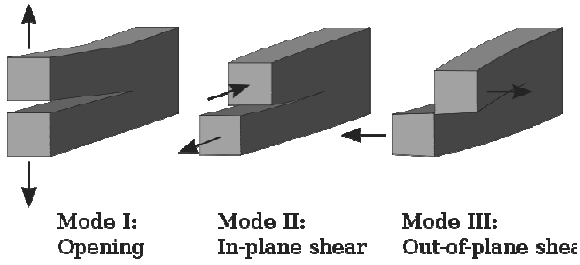

Fig. 2. Mode types of crack loading

Fracture toughness for ceramics is one of the most controversial issues in materials testing, with more than 30 different tests and many variations for each test [6]. Considering a various approach to determine fracture toughness, several meanings of this term have been used: plane strain fracture toughness $K_{IC,}$ strain energy release rate G_{IC}, indentation fracture toughness (sometime called Vickers/Palmqvist toughness). Many methods are currently used to measure fracture toughness of ceramic materials [7,8,9]. The first universally agreed standards for fracture toughness have been existing only since 2003 [10,11,12]. The measurement procedure of fracture toughness is based on the principle of linear-elastic fracture mechanics (LEFM) and contains three main steps: generation of cracks in the test specimen, measurement of the load at failure stress respectively, and crack depth [13]. In the case of ideally brittle materials, the fracture toughness is independent of the crack extension and then flat crack resistance curve (*R*-curve) is obtained. In many ceramics a diverse behaviour is observed. The crack growth resistance increases with the increasing crack extension. Some structural ceramics show an increase of fracture resistance with crack extension under stable crack growth. This phenomenon is called *R-curve* behaviour. The increase of fracture resistance with crack extension may occur due to several effects. The most serious influence is expected by friction at the border of the crack tip, which can cause so-called bridging effects. Further possible reasons for the increase of fracture resistance with crack extension are all energy-consuming effects, for example, crack branching. Another reason for *R-curve* behaviour is constituted by phase transformation effects, which are characteristic of alumina-zirconia ceramics. *R-curve* behaviour of ceramic materials is a desirable mechanical effect. Due to the increase of fracture resistance with crack extension, successive increasing of additional energy is necessary for a crack to propagate until a failure of a ceramic component occurs [14]. The fracture toughness tests generally require a specimen that contains a pre-existing crack, often generated by fatigue pre-cracking. But in the case of the brittle ceramics the fatigue technique is limited to be implemented because of difficulties in arrestment of cracks on

demanded length. The Single-Edge-Notched Beam (SENB) method was developed as a simple and inexpensive alternative, but the results can be influenced by the tip radius of the sawed notch. It seems that for most ceramics presently in use, a notch width of 20 μm or less is necessary to conduct valid tests (Fig. 3). Recently a technique has been introduced to taper a saw cut to a sharp tip radius using a razor blade sprinkled with the diamond paste. This leads to V-notches, hence the name Single-Edge-V-Notched Beam (SEVNB). The most accepted methods specify a precracked specimen loaded to fracture under the three point bending (3PB) - so called conventional methods. These methods of the fracture toughness determination carried out in the three point bending test (3PB) with notched beams require a complex testing procedure and the use of specimens with larger dimensions and complicate geometry.

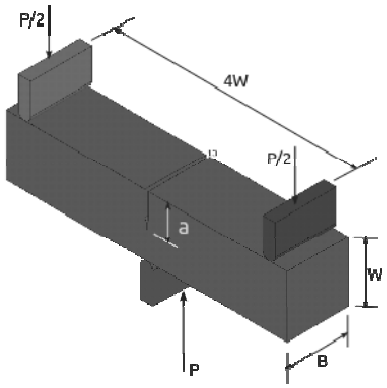

Fig. 3. Single edge notch bending specimen (SENB) specimen for fracture toughness testing

It increases cost and labour consumption of the test. The mentioned difficulties become an inspiration to working out alternative method of fracture toughness measurement by means of the point indentation technique. The indentation technique for a long time long has been considered an attractive method for assessing the toughness of ceramics because of the ease and low cost of conducting experiments. The predominant method to date has involved the use of a Vickers hardness indenter to induce cracks in the ceramics. Such cracks emanate from the indent as a result of residual tensile stresses that develop during unloading. Fracture toughness is calculated from the length of cracks which develop during the Vickers indentation test. The relationship between loading force of indenter and crack length is linear. It is an empirical relationship without a theoretical substructure but indicates a close correlation with mechanical properties of tested materials. As a result of hardness indenter indentation at the ceramic surface a plastic zone beneath the indent is originated according to the elastic-plastic mode. The crack system is generated due to the effect of the plastic deformation zone with surrounding its elastic matrix in the ceramics. Four microcrack morphologies develop in ceramics. Median cracks, radial cracks (a half-penny shaped elliptical crack, much larger than the median crack), lateral cracks (in a plane normal to the median and radial cracks) and Palmqvist radial cracks (originating near the edge of the plastic zone beneath the indent) are observed in ceramics (Figs. 4, 5).

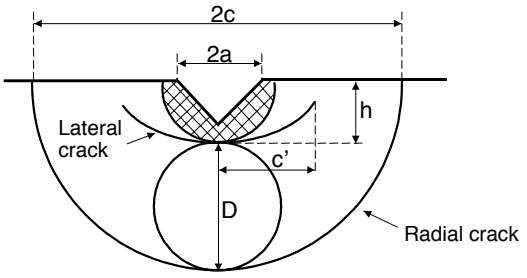

Fig. 4. Crack configuration formed during the indentation toughness test [14]

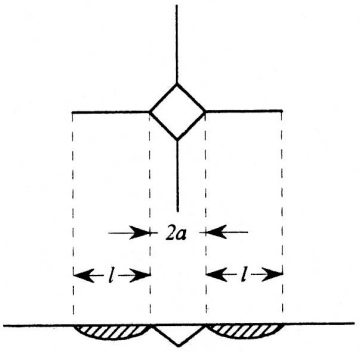

Fig. 5. Palmqvist's cracks formed during the indentation toughness test [15]

Both the Palmqvist and median/radial cracks emanated from the corner of the Vickers hardness indentation provide a base to determinate the indentation fracture toughness.

The lateral cracks are initiated near the base of the plastic deformation zone, below the contact and they spread out laterally on a plane closely parallel to the specimen surface. The literature abounds with various formulas (about 20) for determining the indentation fracture toughness. On the basis of a dimensional analysis of the underlying fracture-mechanical principles and experimental data, it was revealed that the relation between fracture toughness and ratio of crack-to-indent size has an universal behaviour. The variety of cracking mechanism, both the stress field under load and the residual stress field, are clearly very complex. Difficulties of stress analysis have led to some inconsistency in the formulae derived to calculate the indentation fracture toughness. The relation between fracture toughness and the ratio of cracks to indent size at the known Young's modulus and at the condition c/a ≥ 2.5 is expressed by the equation given by Niihara [16] (2):

$$K_{C(HV)}\,\varphi / H\,a^{1/2})\,(H/E\,\varphi)^{2/5} = 0.129\,(c/a)^{-3/2} \qquad (2)$$

where: $K_{C(HV)}$ is the critical stress intensity factor, φ is the constrain factor (φ =3 for alumina ceramics), H is the Vickers hardness, E is the Young's modulus, a - half of indent diagonal.

The primary advantage seen for such a test is the limited volume of material needed and the inexpensive test apparatus.

Furthermore, such a test can be performed in the existing component, with no need to machine a special test piece. In spite of the variety of useful properties of alumina ceramics based on the chemical and thermal stable alpha modification of alumina (α-Al_2O_3), such as: high melting temperature, relatively low density and low thermal conductivity as well as considerable corrosion resistance to the chemically active media at high temperatures, their application as cutting tool inserts, working under mechanical loads and thermal shock conditions, is limited due to brittleness and low strength. One of the methods to improve these properties is to make use of the transformation strengthening process, through the phase transformation of some amount of ZrO_2 introduced into Al_2O_3. The addition of zirconia to alumina allows us to receive zirconia-toughened alumina (ZTA) ceramics, in which strength and toughness have been improved due to the stress induced t-m transformation. The effect of dispersed zirconia grains in an alumina matrix, increasing its mechanical properties, is known as transformation toughening. When stress is applied to the structure, zirconia grains undergo a polymorphous transformation (from tetragonal to monoclinic) in the presence of a growing crack; this transformation results in an increase in volume (3-5%), which leads to a compressive stress field opposing crack propagation. In particular, thanks to its good mechanical properties, zirconia-toughened alumina (ZTA) has widened the scope of application of oxide ceramics and is effectively used in the production of cutting tools, dies or prosthetic components.

Rapid developments in the microstructure of basic ceramics have introduced ceramic-ceramic composites into many engineering applications. It is generally known that Al_2O_3-ZrO_2 composites have better mechanical properties than Al_2O_3 and ZrO_2 because of the dispersion of metastable tetragonal zirconia particles in the alumina matrix, which transform into the stable monoclinic phase under loading. The properties of these materials are determined by their microstructures; therefore, to control their microstructural development and achieve fine microstructures, the sintering parameters must be optimized. On the other hand, the use of metastable zirconia particles as a reinforcing element improves wear resistance through the suppression of crack initiation and propagation due to the higher value of fracture toughness. The transformed particles in the near-surface area induce a compressive stress field, which serves as a toughening mechanism; it reduces the crack-driving force for any existing surface or subsurface cracks [17,18]. On the other hand, pure titanium carbide (TiC) has many attractive properties, such as high hardness, low density, and relatively high thermal and electrical conductivity [19]. Due to great thermodynamic stability, high hardness and compression strength of TiC additive, these ceramic composites have better cutting properties in comparison to oxide ceramics and can be used for the precise machining of hard work-pieces. In this paper, we report a specific characteristic in the fracture toughness measurement of advanced ceramics with particular reference to the α-Al_2O_3, Al_2O_3-ZrO_2, Al_2O_3-ZrO_2-TiC and Al_2O_3-ZrO_2-Ti(C,N) ceramic composites. The aim of this study was to evaluate whether the method is user-friendly, reliable, and most importantly, how well its results compare with indentation methods. High fracture toughness of the structural materials is considered to be an essential property to achieve safety and integrity.

2. Experimental procedure

Different types of alumina matrix composites were used in this study, such as pure alumina α-Al_2O_3 (A), alumina-10 wt% zirconia composite with unstabilized ZrO_2 (A1), alumina-10 wt% zirconia composite with 3 mol% Y_2O_3 stabilized ZrO_2 (A2), alumina-10 %wt zirconia composite with the addition of titanium carbide (B1) and alumina-2 wt% zirconia composite with the addition of titanium carbide-nitride (B2). A high purity alumina powder α-Al_2O_3 > 99.8 wt% type A16SG was produced by the Alcoa firm with an average particle size below 0.5 μm. Pure zirconia was obtained by precipitation from the $ZrOCl_2$ water solution of by means of ammonia water solution. Sintering additives, such as MgO, to inhibit grain growth have been introduced. Specific surface areas S_{BET}=4.54 m^2/g of the alumina particles, pure zirconia S_{BET}=41.3 m^2/g, and 3mol% yttria doped zirconia, S_{BET}=4.70 m^2/g respectively were measured by the BET multipoint method, using N_2 as the adsorption/desorption gas at the temperature of liquid nitrogen. The experiments applied alumina-based composites with the addition of different kind of zirconia, such as zirconia stabilized with 3mol %, in monoclinic phase $ZrO_2^{(m)}$ produced according to own technology carried out in Department of Advanced Ceramics of AGH in Cracow, a mixture of 5 wt% ZrO_2 with modification of the zirconia phase (partially stabilized with 5 wt% Y_2O_3-PYT05.0 (ZY5) produced by Unitec Ceramics, England, with an average particle size of 0.9-1.1 μm. and 2 wt% of the monoclinic phase of zirconia in submicron $ZrO_2^{(m)}$ scale produced by Fluka, Germany. Powder Ti(C,N) grade B.A., produced by H.C. Starck, Germany, was used in experiments. Sintering additives, such as MgO_{nano} (0.3 wt%), were introduced to inhibit grain growth. The initial compositions of compounds selected for testing are presented in Table 1.

Table 1.
Composition of selected compounds

Compound	Compound composition, wt%					
	Al_2O_3	ZY3	ZY5	$ZrO_2^{(m)}$	TiC	Ti(C,N)
	μm	μm	μm	μm	μm	nm
A	100.0	-	-	-	-	-
A1	90.0	-	-	10	-	-
A2	90.0	10	-	-	-	-
B1	85.0	-	5	5	5	-
B2	68.0	-	-	2	-	30

Components were mixed for approximately thirty hours in alumina mills with zirconia balls, with the addition of a plasticizer. Materials, uniformly set, after plasticizing and drying, were granulated. Green compacts of 60.0×70.0×7.0 mm were uniaxially pressed at 50 MPa and then cold isostatically pressed at 250 MPa. Alumina ceramics and alumina-zirconia composites were sintered at a maximum temperature of 1923K at constant heating and cooling rates of the furnace (specimens A, A1, A2). The rest of specimens (B1, B2) with the additions of TiC and

Ti(C,N) were sintered at a high temperature vacuum furnace of the Balzers firm at a temperature beneath 1973 K. After sintering plates were cutting on the beams and next were thinned out to the size 1.5×4.0×50.0±0.1 mm. An initial 0.9 mm deep notch was produced by diamond saw (0.20 mm thick) and then the notch tip was sharpened manually using a razor blade (0.025 mm thick) up to deep 1.1 mm. A sharp crack was propagated from the notch tip when the specimens were subjected to a three-point bending test up to failure. The conventional method bases on three point bending (3PB) of single edge notched beam (SENB) specimens mechanically notched were used. The specimens were loaded with the rate of 1 μm·min^{-1}. For the observation of the *R-curve* the specimens with the wide polished side surface and vacuum evaporated thin aluminium layer (about 150 nm thick) were notched. The controlled crack growth of specimens with a double notch was carried using the Zwick testing machine. Following measurements were performed on the tested specimens: Vickers hardness HV1, fracture toughness at room temperature K_{IC}, Young's modulus, wear resistance v_n (determined by speed of mass loss) and apparent density ρ_p. The SENB specimens (mechanically notched) were used to determine fracture toughness by means of a conventional method based on the three-point bending of specimens (3PB)]. The relationship $K_{IC} = f(c)$ is given by equations (3, 4) [19]:

$$K_{IC} = 1.5\frac{P_c S}{W^2 B} Yc^{1/2} \tag{3}$$

$$Y = \frac{\sqrt{\Pi}}{(1-\beta)^{\frac{3}{2}}}\left[0.3738\beta + (1-\beta)\sum_{i,j=0}^{4} A_{ij}\beta^i\left(\frac{W}{S}\right)^j\right] \tag{4}$$

where: P_c = critical load, S = support span, W= width, B = specimen thickness, Y = geometric function, c = crack length, β = c/W and A_{ij} are the coefficients given by Fett [20].

Modulus of elasticity (Young's modulus) of the tested composites was determined by a measuring the transmission velocity of -longitudinal and transversal ultrasonic waves through the sample using the Panametrics Epoch III ultrasonic flaw detector. The accuracy of calculated Young's modulus was estimated at 2%. Calculations were made using the following formula (5):

$$E = \rho C_T^2 \frac{3C_L^2 - 4C_T^2}{C_L^2 - C_T^2} \tag{5}$$

where: E - Young's modulus, C_L - velocity of the longitudinal wave, C_T - velocity of the transversal wave, ρ - density of the material.

Microstructure observations of the specimen were carried out using the JEOL JSM-6460LV scanning electron microscope. X-ray diffraction was used both to identify phases and to assess the percentage fraction of tetragonal zirconia phase (*t*) and monoclinic zirconia phase (*m*).

3. Results and discussion

The results obtained from the tests concerning apparent density ρ_p, Young's modulus E, Vickers hardness HV1, fracture toughness at room temperature K_{IC}, indentation fracture toughness $K_{IC(HV)}$ of the tested alumina ceramics and alumina matrix composites with various compositions are presented in Table 2.

Table 2.
Selected mechanical properties of tested alumina ceramics and alumina matrix composites

Material	Apparent density ρ_p, g/cm^3	Vickers hardness HV1, GPa	Young's modulus E, GPa	Fracture toughness K_{IC}, MPa·m$^{1/2}$	Indentation fracture toughness $K_{IC(HV)}$, MPa·m$^{1/2}$
A	3.92	18.3	385	3.75	3.72
A1	4.10	18.2	377	4.68	5.00
A2	4.10	18.3	379	4.00	4.17
B1	4.10	18.6	378	4.85	5.20
B2	4.18	18.5	385	4.22	4.30

The tested ceramics exhibit high Vickers hardness HV1 in the range of (18.2-18.6 GPa), similar values of elastic modulus (377-385 GPa), fracture toughness (critical stress intensity factor) K_{IC} in the range of (3.75-4.85) MPa·m$^{1/2}$ and indentation fracture toughness $K_{IC(HV)}$ in the range of (3.72-5.20) MPa·m$^{1/2}$. On the basis of the analysis of the fracture toughness results we can observe that the lowest value of K_{IC} is revealed by pure alumina ceramics. The addition of (10 wt%) unstabilized zirconia to alumina or a small amount (5 wt%) of TiC to alumina-zirconia composite improve K_{IC} by about 20% and 23% respectively in comparison to alumina ceramics. The phase analysis by X-ray diffraction in the Al_2O_3-10wt% ZrO_2 with stabilized and unstabilized zirconia reveals a different volume fraction of the monoclinic zirconia phase in relation to the volume fraction of the tetragonal zirconia phase in these ceramics. In the Al_2O_3-10wt% ZrO_2 with unstabilized ZrO_2 (A1) the volume fraction of the monoclinic zirconia phase in relation to the volume fraction of the tetragonal zirconia phase was about 25%. The Al_2O_3-10wt% ZrO_2 composite with stabilized ZrO_2 (A2) is exhibited only by tetragonal zirconia phase $ZrO_2^{(t)}$. Thus the transformation of polymorphous phases caused toughening of the Al_2O_3-10 wt% ZrO_2 (A1) specimen so the value of fracture toughness is higher for this composite. A similar effect can be observed for the alumina-zirconia composite with the addition of TiC, Fig. 6.

The values of (K_R) were determined for the appropriate crack length *c* during in situ observation of crack propagation at the top of the notch according to formulas 1, 2 (Fig. 7).

On the basis of the obtained data *R-curves* for the tested ceramics were plotted. *R-curves* selected from the batch of specimens are illustrated in Fig. 8. The pronounced character of *R-curve* observed for alumina ceramics generates an increasing dependence on crack growth resistance with crack extension (Fig. 8a). *R-curve* has not been observed for carbide-nitride reinforced composite based on alumina with unstabilized ZrO_2 (Al_2O_3-30 wt% Ti(C,N) with 2 wt% ZrO_2 -specimen B2) Fig. 8b.

An increasing character of *R-curve* for alumina means that the bridging mechanism responsible for the existence of *R-curve* is significant in toughening of these ceramics.

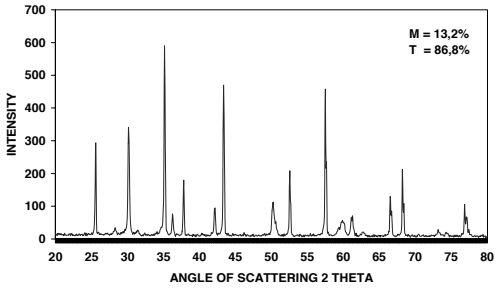

Fig. 6. X-ray diffraction analysis of Al_2O_3-ZrO_2-TiC (B1) alumina ceramic composite

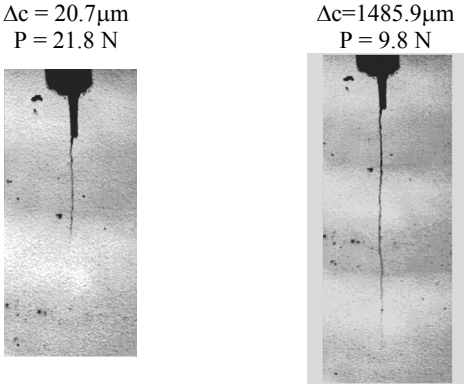

Fig. 7. View of controlled crack growth in a specimen of the Al_2O_3-10wt% ZrO_2 (A1) composite

The microstructure of the alumina ceramics with the bridging effect is presented in Fig. 9. Visible *R-curve* effects were observed in the coarse grain alumina and they diminished in the fine grain alumina.

In the case of ideally brittle materials, the fracture toughness is independent of the crack extension. In this case, a so-called flat crack resistance curve *(R-curve)* is obtained. In the ceramics the development of bridging consists in weak grain-boundary interfaces that serve to deflect the crack around intact grains, leaving them to span the crack. Stress is transmitted across these bridging elements because the friction is enhanced by the presence of local residual stress that results from thermal expansion mismatch between neighbouring grains. The microstructure of the tested ceramics is presented in Figs. 10, 11, 12.

The values of the indentation fracture toughness $K_{IC(HV)}$ of alumina and alumina-10 wt% stabilized zirconia composites are similar to K_{IC} obtained by means of the conventional method. However, the alumina-10 wt% unstabilized zirconia and alumina matrix composites with additions of TiC (specimen B1) show higher values of the $K_{IC(HV)}$ by about 10% in comparison to K_{IC}. Study was conducted for the direct measurements of the Vickers crack length (DCM method) at the 98.1 N loading force applied to the Vickers hardness indenter. Such a loading force guarantees correct Vickers indent without chipping (Fig. 13).

a)

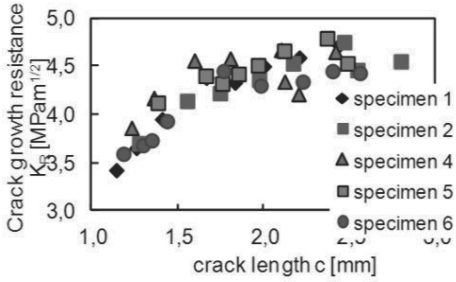

b)

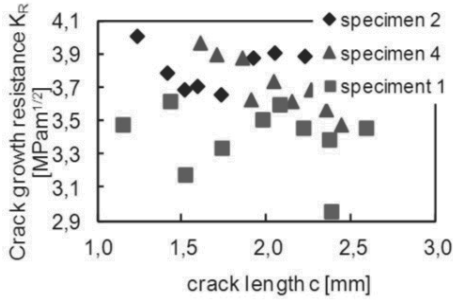

Fig. 8. K_R versus crack length c (*R-curve*) for alumina ceramics: a) Al_2O_3 (A), b) Al_2O_3-30 wt.% Ti(C,N) with 2 wt% ZrO_2 (B2)

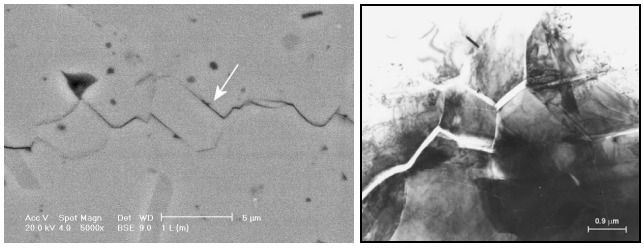

Fig. 9. Microstructure of the alumina ceramics with bridging effect: a) on the specimen's surface indicated by an arrow (SEM micrograph), b) TEM micrograph

a) b)

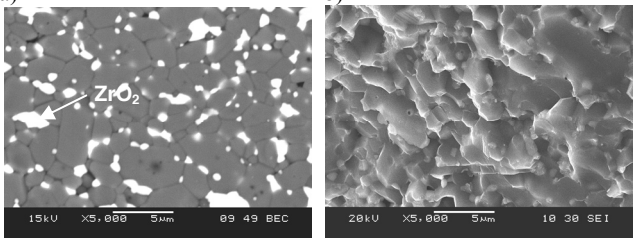

Fig. 10. SEM micrographs of the Al_2O_3-10wt%ZrO_2 ceramic composite (A2): a) surface at 5000x magnification, b) fracture surface at 5 000x magnification

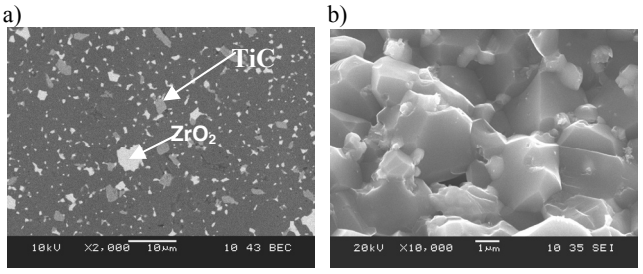

Fig. 11. SEM micrographs of the Al_2O_3-ZrO_2-TiC (B1) alumina ceramic composites specimen: a) surface at 2000x magnification, b) fracture surface at 10000x magnification

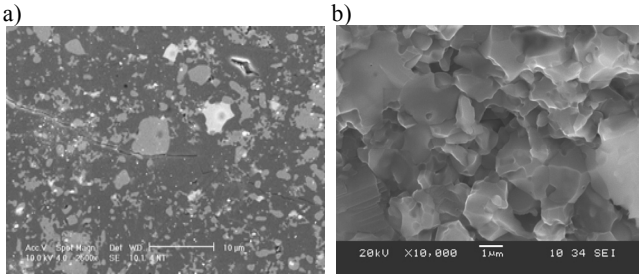

Fig. 12. SEM micrographs of the Al_2O_3-ZrO_2 -Ti(C,N) (B2) alumina ceramic composites specimen: a) surface at 2000x magnification, b) fracture surface at 10 000x magnification

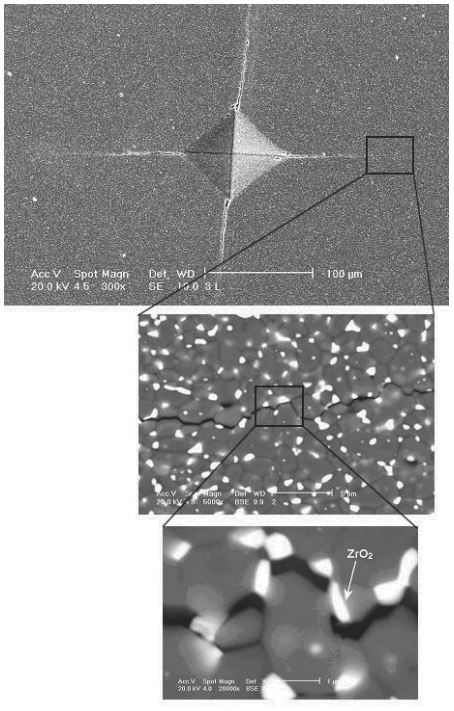

Fig. 13. SEM micrographs of the Vickers indent with crack propagation in the Al_2O_3-10 wt% ZrO_2 (with unstabilized zirconia)-A1 alumina matrix composites specimen produced at indentation load 98.1 N

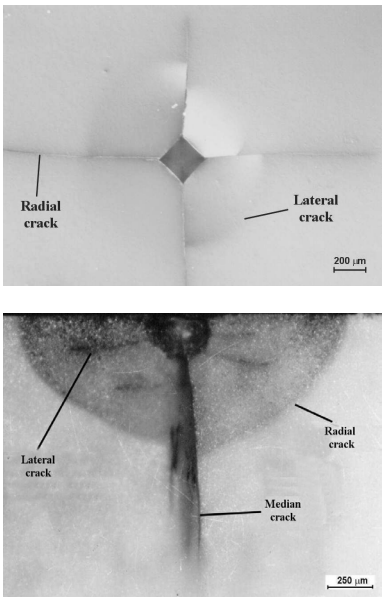

Fig. 14. Examples of cracks in the alumina composites Al_2O_3-10 wt% ZrO_2 (with stabilized zirconia) produced at indentation load 981 N: a) surface micrograph , b) cross-section micrograph

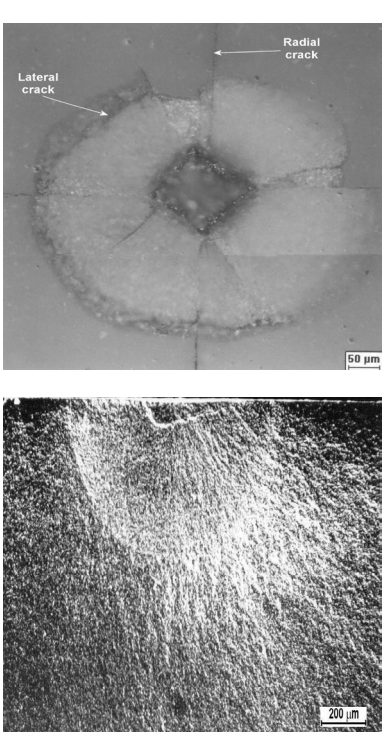

Fig. 15. Examples of cracks in alumina ceramics Al_2O_3: a) produced at indentation load 98.1 N (surface micrograph), b) produced at indentation load 294.3 N (cross-section micrograph)

a)

b)

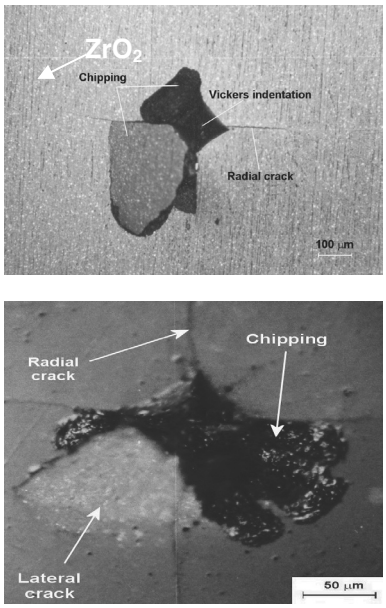

Fig.16. Examples of cracks and chippings in ceramic composites based on alumina produced at indentation load 981 N: a) Al_2O_3-30 wt% Ti(C,N) with 2 wt% ZrO_2, b) Al_2O_3

Serial sectioning was used to determine the indent crack profiles in the samples (Figs. 14, 15). A special staining technique with drop of the saturated lead acetate solution was used to better revealing of the crack profile. The regions on the fracture surfaces were observed using scanning electron microscopy (SEM). The evaluation of chipping compliance of tested ceramics, subjected to different loading forces, was carried by the of Zeiss optical microscope equipped with Dick Nomarski's device (Fig. 16a,b).

The selected equation given by Niihara [16]-formula (2) as being representative was used for the calculations of the indentation fracture toughness, assigned for the specific kind of profile cracks observed on the fracture surface (Figs. 14b, 15b). Tested ceramics exhibit four kinds of cracks: median/radial, Palmqvist and lateral. The crack profile depends on the applied loading force and kind of materials. The change of the loading force in the range from 9.81 N to 981 N causes appearance of diverse crack profiles, starting from Palmqvist cracks up to median/radial and lateral cracks. At the highest loading force for alumina-zirconia composite three kinds of cracks are observed: median/radial and lateral (Fig. 14b).

4. Conclusions

The tested alumina ceramics and alumina matrix composites exhibit high Vickers hardness HV1 in the range of (18.2-18.6) GPa, similar values of elastic modulus (377-385) GPa, fracture toughness (critical stress intensity factor) K_{IC} in the range of (3.75-4.85) MPa·m$^{1/2}$ and indentation fracture toughness $K_{IC(HV)}$ in the range of (3.72-5.20) MPa·m$^{1/2}$. The lowest value of the K_{IC} is revealed by pure alumina ceramics. The addition of (10wt%) unstabilized zirconia to alumina or a small amount (5wt%) of TiC to alumina-zirconia composite improves fracture toughness of these ceramics in comparison to alumina ceramics. Alumina ceramics and alumina-zirconia ceramics reveal the pronounced character of *R-curve* because of an increasing dependence on crack growth resistance with crack extension as opposed to the titanium carbide-nitride reinforced composite based on alumina (Al_2O_3-30 wt% Ti(C,N). with unstabilized 2 wt% ZrO_2. *R-curve* has not been observed for this composite. The increasing character of *R-curve* for the alumina ceramics means that the bridging mechanism responsible for the existence of *R-curve* is significant in toughening of these ceramics. Indentation fracture toughness was determined by means of the direct measurements of the Vickers crack length (DCM method) at the 98.1 N loading force applied to the Vickers hardness indenter. Such a loading force guarantees correct Vickers indent without chipping. The values of the indentation fracture toughness $K_{IC(HV)}$ of alumina and alumina-10 wt% stabilized zirconia composites are similar to K_{IC} obtained by means of the conventional method. The alumina-10 wt% unstabilized zirconia and alumina matrix composites with additions of TiC show higher values of $K_{IC(HV)}$ in comparison to K_{IC} in the range 10%.

References

[1] P. Putyra, M. Podsiadło, B. Smuk, Alumina-Ti(C,N) ceramics with TiB_2 additives, Archives of Materials Science and Engineering 47/1 (2011) 27-32.

[2] L.A. Dobrzański, M. Kremzer, A. Nagel, B. Huchler, Fabrication of ceramic preforms based on Al_2O_3 CL 2500 powder, Journal of Achievements in Materials and Manufacturing Engineering 18 (2006) 71-74.

[3] M. Szutkowska, B. Smuk, Kalinka, K. Czechowski, M. Bućko, M. Boniecki, Selected mechanical properties and microstructure of Al_2O_3-ZrO_2 nanoceramic composites, Journal of Achievements in Materials and Manufacturing Engineering 48/1 (2011) 59-63.

[4] M.D. Demetriou, M.E. Launey, G. Garrett, J. P. Schramm, D.C. Hofmann, W.L. Johnson, W. L. Johnson, R.O. Ritchie, A damage-tolerant glass, Nature Materials 10 (2011) 123-128.

[5] F.T. da Silva, M.A.N. Zacché, H.S. de Amorim, Influence of different surface treatments on the fracture toughness of a commercial ZTA dental ceramic, Materials Res 10/1 (2007) 63-68.

[6] M. Szutkowska, M. Boniecki, Crack Growth Resistance of Alumina Tool Ceramics, Proceedings of the World Congress on "Powder Metallurgy and Particulate Materials" PM2TEC'2002, Orlando, 6 (2002) 34-38.

[7] K. Strecker, S. Ribeiro, M.J. Hoffman, Fracture toughness measurements of LPS-SiC: a comparison of the indentation technique and the SEVNB method, Materials Research 8/2 (2005) 121-124.

[8] G.A. Gogotsi, Fracture toughness of ceramics and ceramic composites, Ceramic International 29 (2003) 777-784.

[9] A. Gatto, Critical evaluation of indentation fracture toughness measurements with Vickers indenter on ceramic matrix composite tools, Materials Processing Technology 174 (2006) 67-73.

[10] ISO 24370:2005, Fine ceramics (advanced ceramics, advanced technical ceramics) - test metod for fracture toughness of monolit hic ceramics at room temperature by chevron-notched beam (CNB) method.
[11] ISO 18756:2003, Fine ceramics (advanced ceramics, advanced technical ceramics) - Determination of fracture toughness of monolit hic ceramics AT room temperature by the surface crack In flexure (SCF) method.
[12] ISO 15732:2005, Fine ceramics (advanced ceramics, advanced technical ceramics) - test method for fracture toughness of monolithic ceramics at room temperature by single edge precracked beam (SEPB) method.
[13] D. Munz , T. Fett, Ceramics, Mechanical properties, Failure behaviour, Materials selection, Springer-Verlag, Berlin Heidelberg, 1999.
[14] M. Szutkowska, M. Boniecki, M. Bucko, R-curve behaviour of alumina matrix ceramics with long cracks, Advances in Science and Technology 45 (2006) 1652-1657.
[15] R. Riedel, Handbook of ceramic hard materials, Wiley-VCH, 2000.
[16] K. Niihara, R. Morena, D. Hasselman, Evaluation of K_{IC} of brittle solid by the indentation method with low crack-to-indent ratios, Journal of Materials Science Letters 1 (1982) 13-16.
[17] G.A. Helvey, Finishing zirconia chairside, What dental technicians need to tell their dentist clients about the effects of surface grinding, Inside dental technology 2/2 (2011) www.dentalaegis.com/idt/2011/02/finishing-zirconia-chairside.
[18] J.F. Bartolome, A.H. De Aza, A. Martın, J.Y. Pastor, J. Llorca, R. Torrecillas, G. Bruno, Alumina/zirconia micro/nanocomposites, A new material for biomedical applications with superior sliding wear resistance, Journal of American Ceramic Society 90/10 (2007) 3177-3184.
[19] Kee-Do Woo, Byung-Ryang Kim, Eui-Pyo Kwon, Duck-Soo Kang, In-Jin Shon, Properties and rapid consolidation of nanostructured TiC-based hard materials with various binders by a high-frequency induction heated sintering, Ceramics International 36 (2010) 351-355.
[20] T. Fett, An analysis of the three-point bending bar by use of the weight function method, Engineering Fracture Mechanics 40/3 (1991) 683-686.